

Dark Matter in the CP-violating NMSSM

Waqas Ahmed^a, Mark Goodsell^b, Shoaib Munir^c

^a *School of Mathematics and Physics, Hubei Polytechnic University,
Huangshi 435003, China*

^b *Laboratoire de Physique Théorique et Hautes Energies (LPTHE),
UMR 7589, Sorbonne Université et CNRS, 4 place Jussieu, 75252 Paris Cedex 05, France*

^c *East African Institute for Fundamental Research (ICTP-EAIFR),
University of Rwanda, Kigali, Rwanda*

waqasmit@hbpu.edu.cn, goodsell@lpthe.jussieu.fr, smunir@eaifr.org

Abstract

In the Next-to-Minimal Supersymmetric Standard Model there is a strong correlation between the mass terms corresponding to the singlet Higgs and the singlino interaction states, both of which are proportional to the parameter κ . If this parameter is complex, explicit CP-violation occurs in the Higgs as well as the neutralino sectors of the model at the tree level, unlike in the minimal scenario. A small magnitude of κ typically yields a $\mathcal{O}(10)$ GeV lightest neutralino with a dominant singlino component. In such a scenario, the phase of κ , beside modifying the properties of the five Higgs bosons, can also have a crucial impact on the phenomenology of the neutralino dark matter. In this study we perform a first investigation of this impact on the relic abundance of the dark matter solutions with sub-100 GeV masses, obtained for parameter space configurations of the model that are consistent with a variety of current experimental data.

1 Introduction

Supersymmetric (SUSY) models with unbroken R -parity provide a viable candidate for the dark matter (DM) of the Universe, in the form of their lightest neutralino. The neutralinos are the mass eigenstates resulting from the mixing of the neutral fermionic superpartners of the electroweak (EW) gauge and Higgs bosons, and have Majorana masses. In the minimal supersymmetric Standard Model (MSSM) [1, 2], which contains two complex Higgs super-multiplets, there are four neutralinos, $\tilde{\chi}_{1,2,3,4}^0$. The interaction strengths of these neutralinos with Standard Model (SM) and SUSY particles are governed by their masses and compositions, i.e., the sizes of their bino, wino and higgsino components.

The two scalar Higgs doublet fields of the MSSM yield a total of five Higgs states. In the limiting case when all the parameters in the Higgs and sfermion sectors are real, these states include two neutral scalars h and H (with $m_h < m_H$), a pseudoscalar A , and a charged pair H^\pm . In any model of new physics, (at least) one neutral scalar, which we generically refer to as the H_{SM} here, ought to have properties consistent with those of the H_{obs} discovered at the Large Hadron Collider (LHC) [3, 4, 5], i.e., a mass near 125 GeV and SM-like coupling strengths. In the MSSM, maximising the tree-level mass of the lighter scalar h , which has an upper limit equal to the Z boson mass, pushes the model into the so-called decoupling limit, where additionally its couplings to the vector bosons mimic those of the H_{obs} . Still, in order for m_h to reach ~ 125 GeV, large loop corrections are needed from mainly the top quark, and its superpartners, the stops [6]. As for the $\tilde{\chi}_1^0$, its consistency with the Planck measurement of the DM relic abundance of the Universe, Ω_h^2 , for a mass below about 1 TeV is only possible if it has a substantial bino component [7, 8].

The Next-to-MSSM (NMSSM) [9, 10, 11, 12] (see, e.g., [13, 14] for reviews) is obtained by adding a Higgs singlet superfield in the MSSM, which results in raising the upper limit on the tree-level mass of the H_{SM} in the model. This reduces the dependence of the H_{SM} mass on the stop sector, and hence alleviates the fine-tuning problem to some extent. Due to the presence of the extra singlet superfield, the neutral Higgs sector of the NMSSM contains three scalars, $H_{1,2,3}$, and two pseudoscalars, $A_{1,2}$. Crucially, in the NMSSM there exists the possibility of the next-to-lightest CP-even Higgs boson, H_2 , acting as the H_{SM} , with the lighter, sometimes even considerably so, H_1 still remaining undetected at the Large Electron Positron (LEP) collider as well as the LHC.

The neutralino sector of the NMSSM also contains a fifth state which, when the lightest of all, can differ significantly from the $\tilde{\chi}_1^0$ of the MSSM in its properties. In particular, in the above-mentioned scenario with the SM-like H_2 , the $\tilde{\chi}_1^0$ typically has a large singlino component, and a mass $\mathcal{O}(10)$ GeV or even lower. Since the H_1 , and generally also the A_1 , lie below ~ 100 GeV [15], this opens up multiple self-annihilation channels for the $\tilde{\chi}_1^0$, which are precluded in the MSSM, in order to generate the correct Ω_h^2 [16, 17, 18, 19, 20]. Potential LHC signatures of such a DM have been studied in [21, 22, 23, 24, 25, 26, 27, 28, 29, 30], and its indirect detection (ID) prospects in [31, 32].

Besides providing one of the leading candidates for low-mass DM, the NMSSM also entertains the possibility of explicit CP-violation in its Higgs sector at the tree level. This could serve as the additional source of CP-violation required for explaining the observed matter-antimatter asymmetry in the Universe through EW baryogenesis [33, 34, 35, 36, 37]. In the SM, the Cabibbo-Kobayashi-Maskawa (CKM) matrix is the lone and insufficient source of CP-violation, while the MSSM Higgs sector can only violate CP at higher orders [38, 39, 40, 41, 42, 43, 44, 45, 46, 47]. The CP-violating phases of the SUSY-breaking Higgs-sfermion-sfermion couplings, $A_{\tilde{f}}$, where f denotes a SM fermion, in the MSSM can be radiatively transmitted to the Higgs sector, but are tightly constrained by the measurements of fermion electric dipole moments (EDMs) [48, 49]. In the NMSSM, if the Higgs self-couplings, λ and/or κ , appearing in the superpotential are complex, the

scalar and pseudoscalar interaction eigenstates mix together to give five neutral CP-indefinite Higgs states; see [50, 51, 52, 53, 54, 55] for recent studies of the NMSSM Higgs sector with CP violation and [56] for a review. We henceforth refer to this model as the cNMSSM.

Several phenomenological scenarios emerging in the cNMSSM Higgs sector that are distinct from the NMSSM with real parameters (rNMSSM) have been studied in [57, 58, 59, 60, 61, 62]. Importantly, the complex κ parameter associated with the singlet superfield also appears in the entry of the neutralino mass matrix that corresponds to the singlino weak eigenstate. The impact of a non-zero phase of κ on the phenomenology of the $\tilde{\chi}_1^0$ DM has not been analysed in literature thus far. In this article, we take a first step in this direction, and investigate how the relic abundance of the $\tilde{\chi}_1^0$ in the cNMSSM is affected by variations in this phase. We focus mainly on the (EW-scale) cNMSSM parameter space configurations that yield a sub-100 GeV DM, which can be predominantly singlino-like. We also test the consistency of these solutions with the most important latest experimental constraints, including the Higgs boson data from the LHC and the electron and neutron EDMs, and study some of their phenomenological implications.

The article is organised as follows. In the next section we briefly revisit the Higgs and neutralino sectors of the cNMSSM. Section 3 contains details of our numerical analysis of the model's parameter space with the focus on the DM observables. In section 4 we present the results of our analysis, and we summarise our findings in section 5.

2 The NMSSM with explicit CP-violation

2.1 The Higgs sector

The superpotential of the NMSSM is written as

$$W_{\text{NMSSM}} = \widehat{U}^C \mathbf{h}_u \widehat{Q} \widehat{H}_u + \widehat{D}^C \mathbf{h}_d \widehat{H}_d \widehat{Q} + \widehat{E}^C \mathbf{h}_e \widehat{H}_d \widehat{L} + \mu \widehat{H}_u \widehat{H}_d + \lambda \widehat{S} \widehat{H}_u \widehat{H}_d + \frac{\kappa}{3} \widehat{S}^3 \quad (1)$$

in terms of the singlet Higgs superfield, \widehat{S} , besides the two $SU(2)_L$ doublet superfields,

$$\widehat{H}_u = \begin{pmatrix} \widehat{H}_u^+ \\ \widehat{H}_u^0 \end{pmatrix}, \quad \widehat{H}_d = \begin{pmatrix} \widehat{H}_d^0 \\ \widehat{H}_d^- \end{pmatrix}, \quad (2)$$

of the MSSM. The above superpotential observes a discrete Z_3 symmetry, which is imposed in order to explicitly break the dangerous $U(1)_{PQ}$ symmetry, and renders it conformal-invariant by forbidding the $\mu \widehat{H}_u \widehat{H}_d$ term present in the MSSM superpotential. Here, the mixing between the H_d^0 field and the H_u^0 fields, necessary for each of them having a non-trivial vacuum expectation value (TeV) at the minimum of the potential, is instead generated by the $\lambda \widehat{S} \widehat{H}_u \widehat{H}_d$ term. This results in a dynamic $\mu_{\text{eff}} \equiv \lambda s / \sqrt{2}$ term when the singlet field acquires a VEV, s , naturally near the SUSY-breaking scale.

The tree-level Higgs potential of the NMSSM is obtained as

$$\begin{aligned} V_0 = & \left| \lambda (H_u^+ H_d^- - H_u^0 H_d^0) + \kappa S^2 \right|^2 \\ & + \left(m_{H_u}^2 + |\lambda S|^2 \right) \left(|H_u^0|^2 + |H_u^+|^2 \right) + \left(m_{H_d}^2 + |\lambda S|^2 \right) \left(|H_d^0|^2 + |H_d^-|^2 \right) \\ & + \frac{g_1^2 + g_2^2}{8} \left(|H_u^0|^2 + |H_u^+|^2 - |H_d^0|^2 - |H_d^-|^2 \right)^2 + \frac{g_2^2}{2} |H_u^+ H_d^{0*} + H_u^0 H_d^{-*}|^2 \\ & + m_S^2 |S|^2 + (T_\lambda (H_u^+ H_d^- - H_u^0 H_d^0) S + \frac{1}{3} T_\kappa S^3 + \text{h.c.}), \end{aligned} \quad (3)$$

where g_1 and g_2 are the $U(1)_Y$ and $SU(2)_L$ gauge couplings. It is customary to define the trilinears proportional to the superpotential couplings as

$$T_\lambda \equiv \lambda A_\lambda, \quad T_\kappa \equiv \kappa A_\kappa. \quad (4)$$

A_λ and A_κ above are the soft SUSY-breaking counterparts of the superpotential couplings, and all of these can very well be complex parameters, with the corresponding phases, $e^{i\phi_{A_\lambda}}$, $e^{i\phi_{A_\kappa}}$, $e^{i\phi_\lambda}$, and $e^{i\phi_\kappa}$.

After spontaneous EW symmetry breaking, V_0 is evaluated at the vacuum, in terms of fields defined around their respective VEVs, v_u , v_d and s , as

$$\begin{aligned} H_d^0 &= \begin{pmatrix} \frac{1}{\sqrt{2}}(v_d + H_{dR} + iH_{dI}) \\ H_d^- \end{pmatrix}, \\ H_u^0 &= e^{i\theta} \begin{pmatrix} H_u^+ \\ \frac{1}{\sqrt{2}}(v_u + H_{uR} + iH_{uI}) \end{pmatrix}, \\ S &= \frac{e^{i\varphi}}{\sqrt{2}}(s + S_R + iS_I). \end{aligned} \quad (5)$$

The potential then contains the phase combinations

$$\phi'_\lambda - \phi'_\kappa \text{ (with } \phi'_\lambda \equiv \phi_\lambda + \theta + \varphi \text{ and } \phi'_\kappa \equiv \phi_\kappa + 3\varphi), \phi'_\lambda + \phi_{A_\lambda}, \text{ and } \phi'_\kappa + \phi_{A_\kappa}.$$

However, assuming vanishing spontaneous phases θ and φ , the last two phase combinations above can be determined up to a twofold ambiguity using the minimisation conditions of V_0 , leaving $\phi'_\lambda - \phi'_\kappa$ as the only physical CP phase (see [59] for more details).

The potential V_0 with complex phases leads to a 5×5 Higgs mass matrix, \mathcal{M}_0^2 , in the $\mathbf{H}^T = (H_{dR}, H_{uR}, S_R, H_I, S_I)$ basis, with the massless Nambu-Goldstone mode rotated away. After including the higher order corrections from various sectors of the model [57, 59, 63], the resulting Higgs mass matrix, $\mathcal{M}_H^2 = \mathcal{M}_0^2 + \Delta\mathcal{M}^2$, is diagonalised using an orthogonal matrix, O , as $O^T \mathcal{M}_0^2 O = \text{diag}(m_{H_1}^2, m_{H_2}^2, m_{H_3}^2, m_{H_4}^2, m_{H_5}^2)$. The masses of the five CP-mixed physical Higgs bosons thus obtained are ordered such that $m_{H_1}^2 \leq m_{H_2}^2 \leq m_{H_3}^2 \leq m_{H_4}^2 \leq m_{H_5}^2$.

2.2 The Neutralino sector

As noted in the Introduction, the fermion component of \widehat{S} , called the singlino, mixes with the neutral gauginos, \widetilde{B}^0 and \widetilde{W}_3^0 , and higgsinos, \widetilde{H}_d^0 and \widetilde{H}_u^0 , to yield five neutralinos in the NMSSM. The symmetric neutralino mass matrix in the gauge eigenstate basis, $\widetilde{\psi}^0 = (-i\widetilde{B}^0, -i\widetilde{W}_3^0, \widetilde{H}_d^0, \widetilde{H}_u^0, \widetilde{S})$, is written as

$$\mathcal{M}_{\widetilde{\chi}^0} = \begin{pmatrix} M_1 & 0 & -m_W \tan \theta_W \cos \beta & m_W \tan \theta_W \sin \beta & 0 \\ 0 & M_2 & m_W \cos \beta & -m_W \sin \beta & 0 \\ -m_W \tan \theta_W \cos \beta & m_W \cos \beta & 0 & -\mu_{\text{eff}} & -\lambda v_u \\ m_W \tan \theta_W \sin \beta & -m_W \sin \beta & -\mu_{\text{eff}} & 0 & -\lambda v_d \\ 0 & 0 & -\lambda v_u & -\lambda v_d & 2\kappa s \end{pmatrix}, \quad (6)$$

with m_W and θ_W being the W -boson mass and the weak mixing angle, respectively. The neutralino masses and compositions at the tree level thus depend on the Higgs-sector parameters λ , κ , μ_{eff} , v_u , v_d and the gaugino masses M_1 and M_2 . When any of these parameters is complex, the mass matrix in eq. (6) can be diagonalised by a unitary matrix N , to give $D = \text{diag}(m_{\widetilde{\chi}_i^0}) = N^* \mathcal{M}_{\widetilde{\chi}^0} N^\dagger$,

for $i = 1 - 5$. The neutralino mass eigenstates are then given by $\tilde{\chi}_i^0 = N_{ij}\tilde{\psi}_j^0$, and are again ordered as $m_{\tilde{\chi}_1^0} \leq m_{\tilde{\chi}_2^0} \leq m_{\tilde{\chi}_3^0} \leq m_{\tilde{\chi}_4^0} \leq m_{\tilde{\chi}_5^0}$.

The $\tilde{\chi}_1^0$, which is the lightest neutral SUSY particle and hence a DM candidate, is given by the linear combination

$$\tilde{\chi}_1^0 = N_{11}\tilde{B}^0 + N_{12}\tilde{W}_3^0 + N_{13}\tilde{H}_d^0 + N_{14}\tilde{H}_u^0 + N_{15}\tilde{S}^0. \quad (7)$$

Thus, the relative sizes of the soft gaugino masses $M_{1,2}$, the μ_{eff} -parameter and the κs term determine whether the $\tilde{\chi}_1^0$ is gaugino-, higgsino- or singlino-like. For example, in the limit $\mu_{\text{eff}} \ll \min[M_1, M_2]$, the term $[\mathcal{M}_{\tilde{\chi}^0}]_{55} = 2\kappa s = 2\frac{\kappa\mu_{\text{eff}}}{\lambda}$ in eq. (6) results in a singlino-dominated $\tilde{\chi}_1^0$ for $2\kappa/\lambda < 1$. Importantly, in SUSY models the charged higgsinos (\tilde{H}_u^+ and \tilde{H}_d^-) and winos (\tilde{W}^+ and \tilde{W}^-) also mix to form the chargino eigenstates, $\tilde{\chi}_a^\pm$ ($a = 1, 2$). The mass matrix for the charginos is given by

$$\mathcal{M}_{\tilde{\chi}^\pm} = \begin{pmatrix} M_2 & \sqrt{2}m_W \sin \beta \\ \sqrt{2}m_W \cos \beta & \mu_{\text{eff}} \end{pmatrix}. \quad (8)$$

This implies that M_2 and μ_{eff} have a lower bound of about 100 GeV, owing to the non-observation of a chargino at the LEP collider. Since no such constraint exists on the M_1 and $2\kappa s$ terms, the $\tilde{\chi}_1^0$ in the NMSSM can have a mass much lower than 100 GeV as long as it is predominantly bino- and/or singlino-like. The presence of a certain amount of higgsino is, however, necessary to obtain a realistic relic abundance.

The existence of the singlino in the NMSSM, even in the absence of the CP-violating phases noted above, leads to some unique possibilities in the context of DM phenomenology, compared to the MSSM. In the limit of large $\tan \beta \equiv v_u/v_d$ and large $m_A \equiv \frac{\lambda s}{\sin 2\beta}(\sqrt{2}A_\lambda + \kappa s)$ (which effectively decouples the doublet-like H_3 and A_2 from the rest of the particle spectrum, so that $m_{A_2} \simeq m_A$), the masses of the two lightest CP-even scalars can be approximated by [64]

$$M_{H_1, H_2}^2 \approx \frac{1}{2} \left\{ m_Z^2 + 4(\kappa s)^2 + \kappa s A_\kappa \sqrt{[m_Z^2 - 4(\kappa s)^2 - \kappa s A_\kappa]^2 + 4\lambda^2 v^2 [2\lambda s - (A_\lambda + \kappa s) \sin 2\beta]^2} \right\}, \quad (9)$$

where $v \equiv \sqrt{v_u^2 + v_d^2}$. Thus the mass of the lighter of these two (when the heavier one is required to be the H_{SM}) scales with κs , as does that of the singlino. At the same time, the mass-squared of the lighter pseudoscalar, which is almost purely a singlet, reduces to

$$m_{A_1}^2 \simeq -3\kappa s A_\kappa. \quad (10)$$

This correlation between the masses of the A_1 and the $\tilde{\chi}_1^0$ implies that they can be naturally close to each other, thus opening the possibility of the former's self-annihilation via the latter. Evidently, while H_1 can also have a mass in the vicinity of m_{A_1} , it is more strongly constrained by Eq. (9) from taking values close to $2\tilde{\chi}_1^0$. Even if it does acquire the correct mass, the $\tilde{\chi}_1^0$ annihilation via s -channel H_1 is p -wave suppressed, which would make its consistency with the thermal relic abundance difficult.

When the CP-violating phases of κ and λ are turned on, they enter the tree-level neutralino mass matrix independently of each other, unlike the combination $\phi'_\lambda - \phi'_\kappa$ of the Higgs sector. In addition, M_1 and M_2 can also be complex parameters, which would be radiatively induced into the Higgs sector at higher orders. Given the composition of the $\tilde{\chi}_1^0$, the size(s) of the most relevant

phase(s) would then affect not only its physical mass, but also its interaction strengths with other particles. Here, our focus on a sub-100 GeV DM, which is also preferably singlino-like (since low-mass bino-like solutions exist in the MSSM too and have been extensively studied), makes ϕ_κ the most obvious choice to investigate the impact of.

2.3 The electric dipole moments of fermions

Beyond the Born approximation, various CP-violating phases are (co-)induced in the Higgs and neutralino sectors of the cNMSSM. Such phases are subject to constraints from the non-observation of the EDMs of the electron and the neutron. The most recent limits on these EDMs read

$$|d_e| < 1.1 \times 10^{-29} e \text{ cm} [65]; \quad |d_n| < 1.8 \times 10^{-26} e \text{ cm} [66]. \quad (11)$$

The limit on the electron EDM above is based on the thorium monoxide experiment, and is more stringent than the one from the HfF^+ experiment [67]. In SUSY models, the one-loop EDMs of the charged leptons and the light quarks are induced by chargino and neutralino exchange diagrams. These should in principle constrain the CP-violating phases of M_1 , M_2 , λ and κ , appearing in the chargino/neutralino sectors at the tree level. In the SUSY spectrum generator code used for our analysis, details of which will be provided in the next section, calculation of the one-loop contributions to d_e and d_n , as well as to d_τ , in the cNMSSM is currently implemented. Note that additional constraints also come from mercury [68] and thallium [69] EDMs, but these can generally be evaded if the masses of the first two generations of squarks are taken to be sufficiently heavy, as discussed in [50].

At the two-loop level, the Higgs-mediated Barr-Zee type diagrams can also contribute significantly to the electron and neutron EDMs. However, several studies have shown that even when these two-loop effects are taken into account, the phase ϕ'_κ is very weakly constrained by the fermionic EDMs [57, 70, 71, 60], especially for smaller values of $|\kappa|$. This is in contrast with the other phases, especially $\phi_{A_{\bar{f}}}$ (the phases of the Higgs-sfermion-sfermion trilinear couplings), which enter the Higgs sector at the one-loop level. Therefore, besides the reason noted above, we choose the ϕ'_κ as the sole representative CP-violating phase additionally to minimise the potential impact of these two-loop diagrams, which are not accounted for in our numerical code. Implementation of the complete set of contributions to the EDMs in our numerical code would go beyond the scope of this article, which aims to explore the DM properties when a non-zero phase appears in the neutralino sector.

3 Numerical Analysis

The radiative corrections to the tree-level Higgs and neutralino mass matrices make the parameters of the other model sectors highly relevant also. However, on the one hand, the NMSSM with grand-unification-inspired boundary conditions is very tightly constrained by the current experimental results, and on the other hand, the most general NMSSM contains more than a hundred free parameters defined at the EW scale. Thus, in order to draw inferences for a particular sector of the model, it is imperative to make multiple assumptions about the free parameters that only impinge at higher orders.

For our numerical analysis, we therefore adopted the following (universality) conditions to

impose on the parameter space of the Z_3 -symmetric cNMSSM at the EW scale:

$$M_{\tilde{f}} \equiv M_{Q_{1,2,3}} = M_{U_{1,2,3}} = M_{D_{1,2,3}} = M_{L_{1,2,3}} = M_{E_{1,2,3}},$$

$$T_{\tilde{f}} \equiv T_{\tilde{t}} = T_{\tilde{b}} = T_{\tilde{\tau}},$$

where $M_{Q_{1,2,3}}^2$, $M_{U_{1,2,3}}^2$, $M_{D_{1,2,3}}^2$, $M_{L_{1,2,3}}^2$ and $M_{E_{1,2,3}}^2$ are the squared soft masses of the sfermions. The (less-often used) parameter $T_{\tilde{f}}$ corresponds to sfermion trilinear couplings; usually these are taken to be proportional to the Yukawas, such that $T_{\tilde{t}}^{ij} = Y_u^{ij} A_{\tilde{t}}$, where i, j are generation indices. In our numerical code, we specified $T_{\tilde{f}}$ directly at the low scale. We fixed all the elements of $T_{\tilde{f}}$ to small values (1 GeV for the diagonal terms and zero otherwise), except for $T_{\tilde{b}}^{(3,3)} = T_{\tilde{t}}^{(3,3)} = T_{\tilde{b}}^{(3,3)} = T_{\tilde{\tau}}^{(3,3)}$, which we left as a free parameter to be scanned over an extended range. The reason for this was to increase the probability of the consistency of $m_{H_{\text{SM}}}$, the dominant corrections to which increase proportionally to $(A_{\tilde{t}} - \mu_{\text{eff}} \cot \beta)^2$, with $m_{H_{\text{obs}}}$. We likewise scanned over wide ranges of M_1 and M_2 to allow maximal possible variations in the $\tilde{\chi}_1^0$ composition. On the other hand, $M_{\tilde{f}}$ and M_3 were fixed to sufficiently large values of 2 TeV and 3 TeV, respectively, so that the sfermions and the gluino could evade the direct search limits from the LHC.

As for the CP-violating phases, in light of the discussion in the previous section, we fixed $\phi'_\lambda = \phi_{M_1} = \phi_{M_2} = \phi_{T_{\tilde{f}}} = \varphi = \theta = 0$ (so that $\phi'_\kappa = \phi_\kappa$). However, the quantities that we choose for the solution of the (five independent) tadpole equations are

$$m_{H_d}^2, m_{H_u}^2, m_S^2, \text{Im}(T_\kappa), \text{Im}(T_\lambda).$$

The first three of these are standard choices familiar from the rNMSSM. However, once we break CP we have two additional non-trivial tadpole equations that must be satisfied, and it is logical to choose the complex part of the trilinear parameters, since these lead to the smallest impact on the spectrum and their magnitude will only be proportional to the violation of CP. With the only non-zero CP-violating phase being ϕ_κ , this leads to

$$\text{Im}(T_\lambda) = \mu_{\text{eff}} \text{Im}(\kappa) - \frac{\sqrt{2}}{sv_u} \text{Re} \left(\frac{\partial \Delta V_0}{\partial H_{dI}} \right),$$

$$\text{Im}(T_\kappa) = \frac{3\lambda v_d v_u}{\sqrt{2}s} \text{Im}(\kappa) + \frac{\sqrt{2}}{s^3} \text{Re} \left(s \frac{\partial \Delta V_0}{\partial S_I} - v_d \frac{\partial \Delta V_0}{\partial H_{dI}} \right). \quad (12)$$

As briefly noted in Sec. 2.1, the real parts of these trilinears are fixed as inputs:

$$\text{Re}(T_\lambda) = \text{Re}(\lambda A_\lambda),$$

$$\text{Re}(T_\kappa) = \text{Re}(\kappa A_\kappa), \quad (13)$$

where now A_λ, A_κ are taken to be real. This means that at the tree level both the trilinear couplings pick up phases from the phase of κ (which are, however, small for $A_\lambda \gg \mu_{\text{eff}}$ and $A_\kappa \gg v_d v_u / s$, and are modified at the higher orders).

To generate the particle spectrum for a given configuration of the final set of the free parameters,

$$|M_1|, |M_2|, |T_{\tilde{f}}|, \tan \beta, |\lambda|, |\kappa|, \mu_{\text{eff}}, A_\lambda, A_\kappa, \phi_\kappa,$$

we incorporated the cNMSSM into the public fortran code **SPheno-v4.0.4** [72, 73] using the Mathematica package **SARAH-v4.14.4** [74, 75, 76, 77, 78, 50, 79].¹ Besides the mass spectrum, **SPheno**

¹We note that **nmssmtools** provides a spectrum generator capable of handling CP violation [63] that contains a less accurate computation of the Higgs masses; whereas **nmssmcalc** [80] provides an equivalent computation of the Higgs masses [55].

also computes the decay widths and branching ratios (BRs) of the Higgs and SUSY particles (at one loop for CP-conserving models [81], but at leading order only for CP-violating ones), as well as a multitude of flavour and other low-energy observables. We linked `SPheno` with the public program `MultiNest-v3.7` [82] for generating output files for sampled configurations of the free parameters from their defined ranges. Multiple scans were performed, with each one corresponding to ϕ_κ fixed to one of the five selected values: 0° (the CP-conserving case, i.e., the rNMSSM but with the five Higgs bosons ordered by their masses, irrespective of their CP-identities), 30° , 60° , 135° , and 180° .² In order to calculate $\Omega_{\tilde{\chi}_1^0} h^2$ and other DM observables for each sampled parameter space point, we also produced a `CalcHEP` [83] model file for the cNMSSM with `SARAH`, which was then embedded in the public code `MicrOmegas-v5.2.4` [84, 85, 86].

The purpose of these scans was to find parameter space points for which

1. Either H_2 or H_3 had a mass in the 122–128 GeV range (thus allowing a theoretical uncertainty of ± 3 GeV around the - assumed - experimental central value of $m_{H_{\text{SM}}} = 125$ GeV). This implied that there would at least be one light Higgs boson available for potential s -channel annihilation of the DM.
2. The H_{SM} (whether H_2 or H_3) had the $\gamma\gamma$, ZZ , $\tau\tau$ and $b\bar{b}$ effective couplings lying within ± 0.2 units of the SM expectation of 1.³
3. The theoretical predictions of the following B -physics observables lied within 2σ deviation from their quoted experimental values.
 - $\text{BR}(B \rightarrow X_s \gamma) \times 10^4 = 3.32 \pm 0.15$ [89],
 - $\text{BR}(B_u \rightarrow \tau^\pm \nu_\tau) \times 10^4 = 1.06 \pm 0.19$ [89],
 - $\text{BR}(B_s \rightarrow \mu^+ \mu^-) \times 10^9 = 3.0 \pm 0.85$ [90].
4. None of the five Higgs states were excluded by the limits from the LEP, TeVatron and LHC searches implemented within the program `HiggsBounds-v5.2.0` [91].
5. The $|d_e|$ and $|d_n|$ satisfied the experimental upper bounds given in eq. (11).
6. The relic abundance of the $\tilde{\chi}_1^0$ never exceeds +10% of the Planck measurement of $\Omega h^2 = 0.119$ [92]. Note that `MultiNest` performs a multimodal sampling of a model’s parameter space based on Bayesian evidence estimation. Our purpose for using this package was simply to scan the parameter space in a more efficient way than random sampling, rather than to draw Bayesian inferences about it. To this end, we defined a Gaussian likelihood function with a peak at $\Omega_{\tilde{\chi}_1^0} h^2 = 0.119$ and a width of $\pm 10\%$ of this value in `MultiNest`. Evidently, the scan collected a number of points far away from the peak also. From these, we removed all the points with $\Omega_{\tilde{\chi}_1^0} h^2 > 0.131$, but retained also the ones for which $\Omega_{\tilde{\chi}_1^0} h^2 < 0.107$ so as to accommodate alternative possibilities, such as non-thermal $\tilde{\chi}_1^0$ production [93] or multi-component DM [94].

²We ignored $\phi_\kappa > \pi$, since we expected the real part of κ to be dominant by far, and hence the overall behaviors of the calculated observables to be approximately symmetric around $\phi_\kappa = \pi$. This was nevertheless verified numerically for the sample value of $\phi_\kappa = 300^\circ$.

³While it is in principle possible to constrain these couplings using the latest combined measurements from the LHC (e.g., [87]) using a program like `HiggsSignals-2` [88] instead we chose (for simplicity) to allow up to 20% deviation from the SM values. The figure of 20% corresponds roughly to the experimentally quoted uncertainties (we also checked that using a smaller value negligibly impacted our results); we were concerned that a combination was overly pessimistic regarding finding valid points, and not primarily concerned with tweaking the (heavier) H_{SM} which otherwise plays little role in the dark matter properties.

Parameter	M_1 (GeV)	M_2 (GeV)	$T_{\tilde{f}}$ (GeV)	$\tan \beta$	
Range	[1, 1000]	[100, 2000]	[-7000, -2000]	[1, 20]	
Parameter	λ	κ	μ_{eff} (GeV)	A_λ (GeV)	A_κ (GeV)
Range	[0.1, 0.7]	[0.001, 0.3]	[100, 500]	[500, 3000]	[\mp 500, 0]

Table 1: Scanned ranges of the cNMSSM parameters. Separate scans were run for ϕ_κ chosen from $\{0^\circ, 30^\circ, 60^\circ, 135^\circ, 180^\circ\}$.

Parameter	TP1	TP2	TP3	TP4	Parameter	TP1	TP2	TP3	TP4
M_1 (GeV)	42	386	689	952	ϕ_κ (degrees)	30	30	30	60
M_2 (GeV)	1967	1565	1273	673	Ωh^2	0.130	0.127	0.119	0.095
$T_{\tilde{f}}$ (GeV)	-2688	-3414	-3938	-4132	$m_{\tilde{\chi}_1^0}$ (GeV)	41	20	6	43
$\tan \beta$	13.69	10.80	14.82	6.84	$m_{\tilde{\chi}_2^0}$ (GeV)	463	251	216	334
λ	0.227	0.323	0.659	0.237	$m_{\tilde{\chi}_3^0}$ (GeV)	469	265	228	351
$ \kappa $	0.178	0.012	0.003	0.015	$m_{\tilde{\chi}_4^0}$ (GeV)	723	393	688	706
μ_{eff}	458	252	192	340	$m_{\tilde{\chi}_5^0}$ (GeV)	1973	1578	1292	948
A_λ (GeV)	2694	2613	2904	2165	$m_{\tilde{\chi}_1^\pm}$ (GeV)	466	256	193	338
A_κ	-11.70	-2.44	-57.45	-31.06	$m_{\tilde{\chi}_2^\pm}$ (GeV)	1988	1597	1310	714
					m_{h_1} (GeV)	87	16	14	34
					m_{h_2} (GeV)	125	45	69	51
					m_{h_3} (GeV)	720	124	127	124
					m_{h_4} (GeV)	4302	2671	2970	2247
					m_{h_5} (GeV)	4302	2672	2974	2247
					m_{H^\pm} (GeV)	4303	2651	2830	2243

Table 2: The input parameters and the spectra for the four selected test points.

4 Low-mass DM in the cNMSSM

The scanned ranges of the nine free parameters (after fixing ϕ_κ) of the cNMSSM are given in Table 1. Evidently, these ranges cannot entail all possible configurations. They are, however, guided by some previous studies [15, 25, 27], and are extensive enough to fulfill the necessary conditions for this analysis, i.e., of yielding a H_2 or H_3 with a mass around 125 GeV, and a sub-100 GeV singlino/bino-dominated $\tilde{\chi}_1^0$. The upper cutoffs on the values of λ and κ are imposed to avoid the Landau pole. A_0 can in principle be both positive and negative, with a marginally different impact on the physical mass of the SM-like Higgs boson for an identical set of other input parameters in each case. Our purpose for using only its negative range was to enhance the efficiency of the numerical scanning code. Note that, at the EW scale κ and A_κ are conventionally taken to be > 0 and < 0 , respectively, in order to prevent negative mass-squared of the lightest pseudoscalar – see Eq.(10). But here, for $90^\circ < \phi_\kappa < 180^\circ$, the real part of κ becomes negative, and hence A_κ ought to be positive. Thus in the scans corresponding to $\phi_\kappa = 135^\circ$ and 180° , A_κ was scanned over positive values only.

The left panel of Fig. 1 shows that a large number of parameter space points meeting all the conditions outlined in the previous section are ruled out by the latest limits on the cross section of the spin-independent DM-proton scattering, σ_{SI}^p , from the XENON-1T experiment [95]. The right

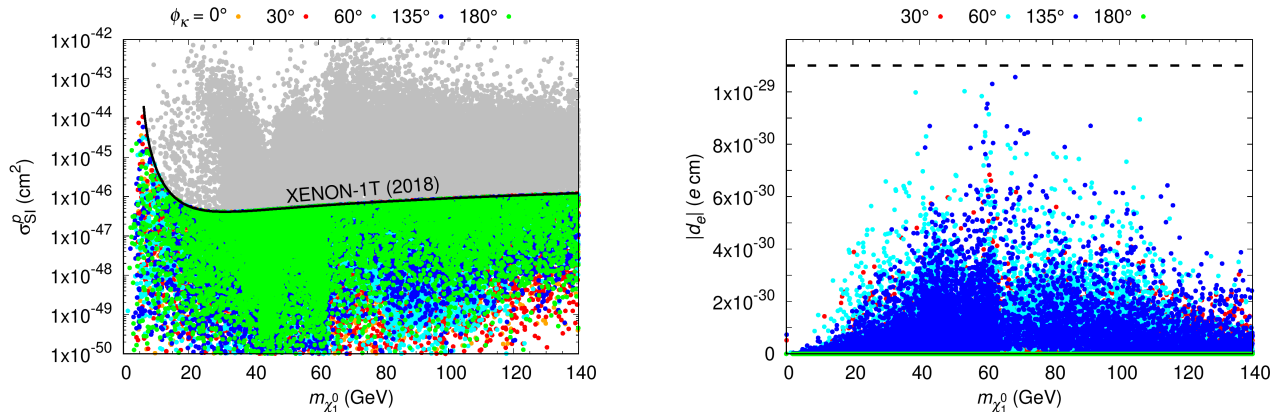


Figure 1: The spin-independent DM-proton cross section (left) and the electron EDM (right) as functions of the DM mass. Different colours of the points illustrate different values of ϕ_κ , and the solid and dashed lines in the left and right panels, respectively, correspond to the experimental limits.

panel confirms the fact that ϕ_κ is indeed very weakly constrained by the one-loop contributions to $|d_e|$, since for almost all the successful scanned points its model prediction lies well below the experimental bound.

In Fig. 2 the $\tilde{\chi}_1^0$ relic abundance is plotted as a function of its mass, separately for points from each scan with fixed ϕ_κ . The grey points in the background are the ones excluded by the XENON-1T limits. In the top-left panel, corresponding to the CP-conserving case, $\Omega_{\tilde{\chi}_1^0} h^2$ is generally quite small, except near $m_{\tilde{\chi}_1^0} \sim m_Z/2$ and $m_{\tilde{\chi}_1^0} \sim m_{H_{SM}}/2$ for the $H_{SM} = H_3$ scenario (blue points), where a few points show consistency with the Planck measurement within $\pm 10\%$. A narrow peak of points also appears around $m_{\tilde{\chi}_1^0} \sim 10$ GeV, where, as we will see later, a very singlino-like $\tilde{\chi}_1^0$ can undergo just the right amount of self-annihilation via the singlet A_1 . Recall that all the five Higgs bosons are ordered by mass and not distinguished by their CP-assignment, and thus the H_1 in the cNMSSM can be either one of the H_1 or A_1 of the rNMSSM. In the $H_{SM} = H_2$ scenario (red points) the correct $\Omega_{\tilde{\chi}_1^0} h^2$ can be obtained for a wide range of $m_{\tilde{\chi}_1^0}$, when it is near either $m_{H_2}/2$ or, more frequently, $m_{H_3}/2$. For $\phi_\kappa = 30^\circ$, in the top-right panel, a few points with $m_{\tilde{\chi}_1^0}$ between 10–20 GeV also appear within (or just outside) the Planck band (i.e., $\Omega h^2 = 0.119 \pm 10\%$). This is not the case for the CP-conserving case above, although the overall picture looks very similar, and is a result of the slight modification in the $\tilde{\chi}_1^0$ composition owing to the CP-violating phase.

When ϕ_κ is increased to 60° (centre-left panel) some Planck-consistent points show up also around $m_{\tilde{\chi}_1^0} = 30$ GeV. Most notably, however, it is possible to obtain the correct $\Omega_{\tilde{\chi}_1^0} h^2$ for the entire ~ 5 –40 GeV mass range when the sign of κ (and hence also of A_κ) is flipped, as demonstrated by the centre-right and bottom-left panels corresponding to $\phi_\kappa = 135^\circ$ and $\phi_\kappa = 180^\circ$, respectively. In fact, for the latter phase, a sole point appears within the Planck band for $m_{\tilde{\chi}_1^0} \simeq 45$ GeV. This is not observed for any of the other selected phases in this figure, but, as we will see below, it is achievable for another point near $\phi_\kappa = 30^\circ$ also. The bottom-right panel presents a holistic picture, where one sees that nearly the entire sub-100 GeV range of $m_{\tilde{\chi}_1^0}$ with $\Omega h^2 = 0.119 \pm 10\%$ is covered by the good points from all of the scans.

For a closer analysis of the impact of the variation in ϕ_κ on $m_{\tilde{\chi}_1^0}$ and its relic abundance, we

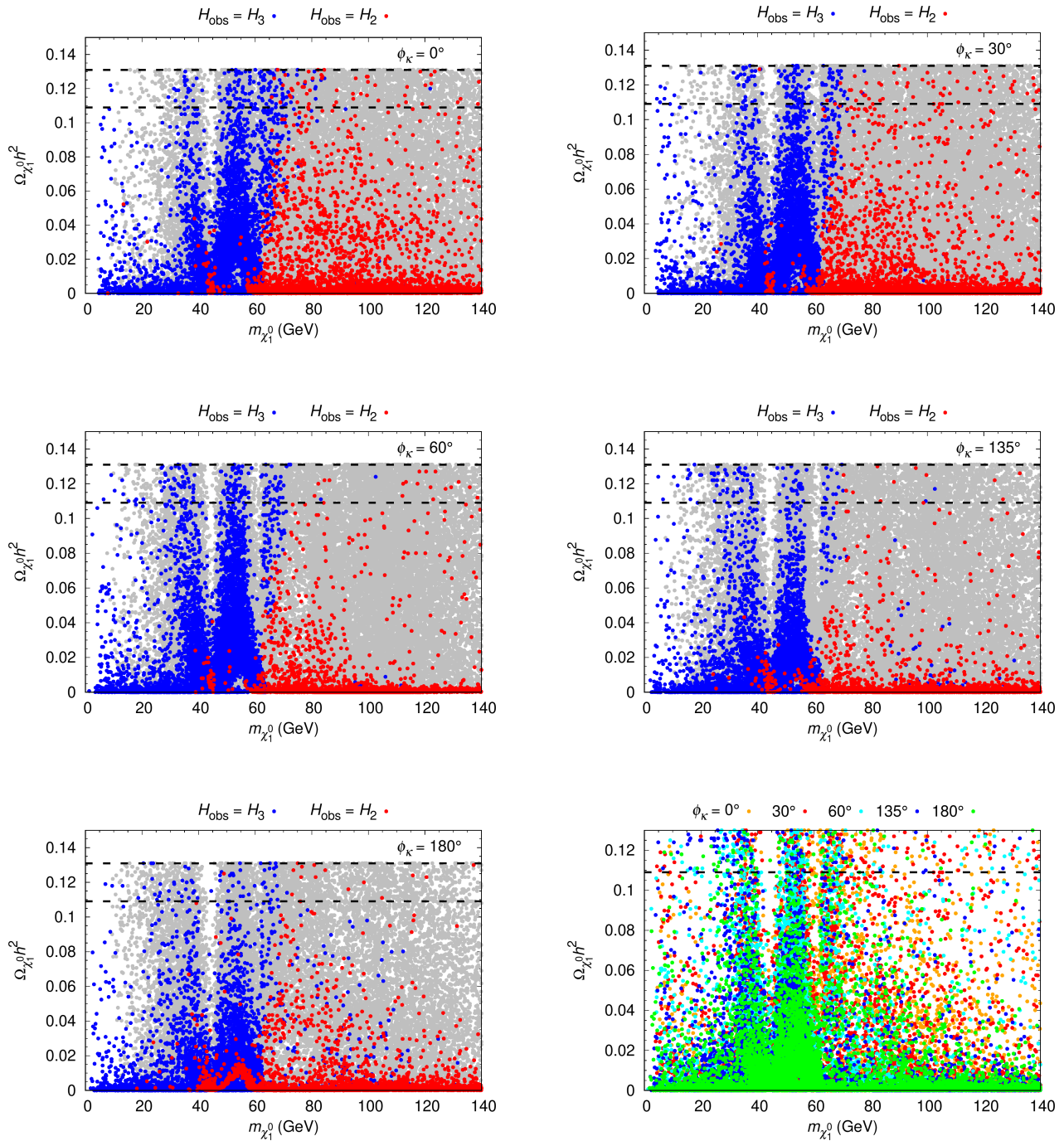


Figure 2: Relic abundance of the DM as a function of its mass, for points obtained from the scans with ϕ_κ fixed to 0° (top-left), 30° (top-right), 60° (centre-left), 135° (centre-right), and 180° (bottom-left). The red points correspond to the $H_{\text{SM}} = H_2$ scenario and the blue points to the $H_{\text{SM}} = H_3$ one. The grey points in the background are the ones ruled out by the XENON-1T limits on σ_{SI}^p . The bottom-right panel shows the allowed points from all the other panels overlapped.

selected four test points (TPs) from among those corresponding to $\phi_\kappa = 30^\circ$ and 60° . The values of the corresponding scanned parameters, along with spectra for one chosen value of ϕ_κ , are given in Table 2. For each of these TPs, $m_{\tilde{\chi}_1^0}$ is plotted as a function of ϕ_κ in all the panels of Fig.3. The heat map in the left column of the figure corresponds to m_{H_1} , in the central column to m_{H_2} , and in the right column to the singlino fraction, N_s , of the $\tilde{\chi}_1^0$. The non-existence of a point for some values of ϕ_κ in a given panel implies that SPheno did not produce an output on account of there being unphysical loop-corrected masses for some particles. The grey points imply inconsistency with one of the constraints 1–5 listed in section 3, while the coloured circles give $\Omega_{\tilde{\chi}_1^0} h^2 > 0.131$. The coloured boxes instead mean $\Omega_{\tilde{\chi}_1^0} h^2 < 0.131$ for that point, and a cross around a box reflects that $\Omega_{\tilde{\chi}_1^0} h^2$ lies within the Planck band, in addition to passing all the constraints.

The TP1 in the top row of Fig.3 is the single (red) point for the $H_{\text{SM}} = H_2$ scenario with $m_{\tilde{\chi}_1^0} \sim 40$ GeV appearing within the Planck band for $\phi_\kappa = 30^\circ$. It does so, however, only for this specific value of ϕ_κ . For almost the entire remaining range of the phase, this parameter space configuration is inconsistent with at least one of the enforced experimental constraints. According to the right panel of this row, the $\tilde{\chi}_1^0$ in TP1 has a negligible singlino component, but is instead entirely bino-like, with a small higgsino fraction just enough for the correct amount of its self-annihilation via the Z boson for $\phi_\kappa = 30^\circ$.

The remaining three TPs belong to the $H_{\text{SM}} = H_3$ scenario. For TP2 also, the Planck-consistent amount of self-annihilation of the $\tilde{\chi}_1^0$, via the H_2 , occurs only for ϕ_κ a few degrees around 30° . $m_{\tilde{\chi}_1^0}$ and m_{H_2} both reduce with increasing ϕ_κ - the latter much slower than the former - until tachyonic masses appear in the particle spectrum for $\phi_\kappa \geq 80^\circ$. The right panel shows that the very large N_s in the CP-conserving case also falls sharply with increasing ϕ_κ , with the Planck-consistency occurring when it is just above 90%. In the case of TP3, as with the TP1, $\Omega_{\tilde{\chi}_1^0} h^2 = 0.119 \pm 10\%$ is satisfied only for $\phi_\kappa = 30^\circ$, when the sharply falling m_{H_1} gets very close to $2m_{\tilde{\chi}_1^0} \simeq 12$ GeV, as seen in the left panel of the third row. Beyond this value of ϕ_κ , the $\Omega_{\tilde{\chi}_1^0} h^2$ drops for a few degrees, owing to excessive annihilation, before rising above the Planck bound again when m_{H_1} grows too small. From the right panel for this TP, the N_s stays almost constant over the entire range of ϕ_κ .

Finally, TP4 is a representative point of the case when the $\Omega_{\tilde{\chi}_1^0} h^2$ falls within the Planck band for $m_{\tilde{\chi}_1^0}$ close to 45 GeV, as hinted earlier. For this TP, taken from among the good points for $\phi_\kappa = 60^\circ$ in Fig. 2, $\Omega_{\tilde{\chi}_1^0} h^2$ originally lies much below the Planck band. However, as the mass of $\tilde{\chi}_1^0$ and its singlino fraction increase (slowly and sharply, respectively) with decreasing ϕ_κ , its Z -mediated annihilation gradually reduces. It reaches a level sufficient to give the correct $\Omega_{\tilde{\chi}_1^0} h^2$ starting from $\phi_\kappa \sim 30^\circ$ all the way to 0° .

In Fig.4 we take a brief look at the BRs of the H_{SM} into $\tilde{\chi}_1^0 \tilde{\chi}_1^0$ (left column), $H_1 H_1$ (central column), and $H_2 H_2$ (right column), for the TPs 1–4 (top row to bottom row), in a bid to understand the implications of different ϕ_κ for the H_{SM} phenomenology at the LHC. For the allowed values of ϕ_κ for TP1, $\text{BR}(H_2 \rightarrow \tilde{\chi}_1^0 \tilde{\chi}_1^0)$ and $\text{BR}(H_2 \rightarrow H_1 H_1)$ are insignificant. In the case of TP2, the $\text{BR}(H_3 \rightarrow \tilde{\chi}_1^0 \tilde{\chi}_1^0)$ rises with increasing ϕ_κ , but does not exceed 4%, while $\text{BR}(H_3 \rightarrow H_1 H_1)$ drops, from about 12% in the CP-conserving case to about 8% for $\phi_\kappa = 80^\circ$. This implies that the prospects of observing the 4-body final state resulting from $H_{\text{SM}} \rightarrow H_2 H_2$ decay reduce significantly as the amount of CP-violation increases. The $\text{BR}(H_{\text{SM}} \rightarrow H_2 H_2)$ varies negligibly.

For TP3, the $\text{BR}(H_3 \rightarrow \tilde{\chi}_1^0 \tilde{\chi}_1^0)$, and hence the invisible decay width of the H_{SM} , rises noticeably with ϕ_κ (while $m_{\tilde{\chi}_1^0}$, given by the heat map, drops), until it reaches the maximum of about 10% for 180° . The $\text{BR}(H_3 \rightarrow H_1 H_1)$ for this TP also falls slowly, as in the case of TP2, while the $H_3 \rightarrow H_2 H_2$ decay is kinematically forbidden. In the case of TP4, again the $\text{BR}(H_3 \rightarrow \tilde{\chi}_1^0 \tilde{\chi}_1^0)$ stays insignificant for all ϕ_κ . On the other hand, the $\text{BR}(H_3 \rightarrow H_1 H_1)$ drops much more sharply compared even to TP2, from about 11% for $\phi_\kappa = 0^\circ$ to about 1% for $\phi_\kappa = 180^\circ$, while the

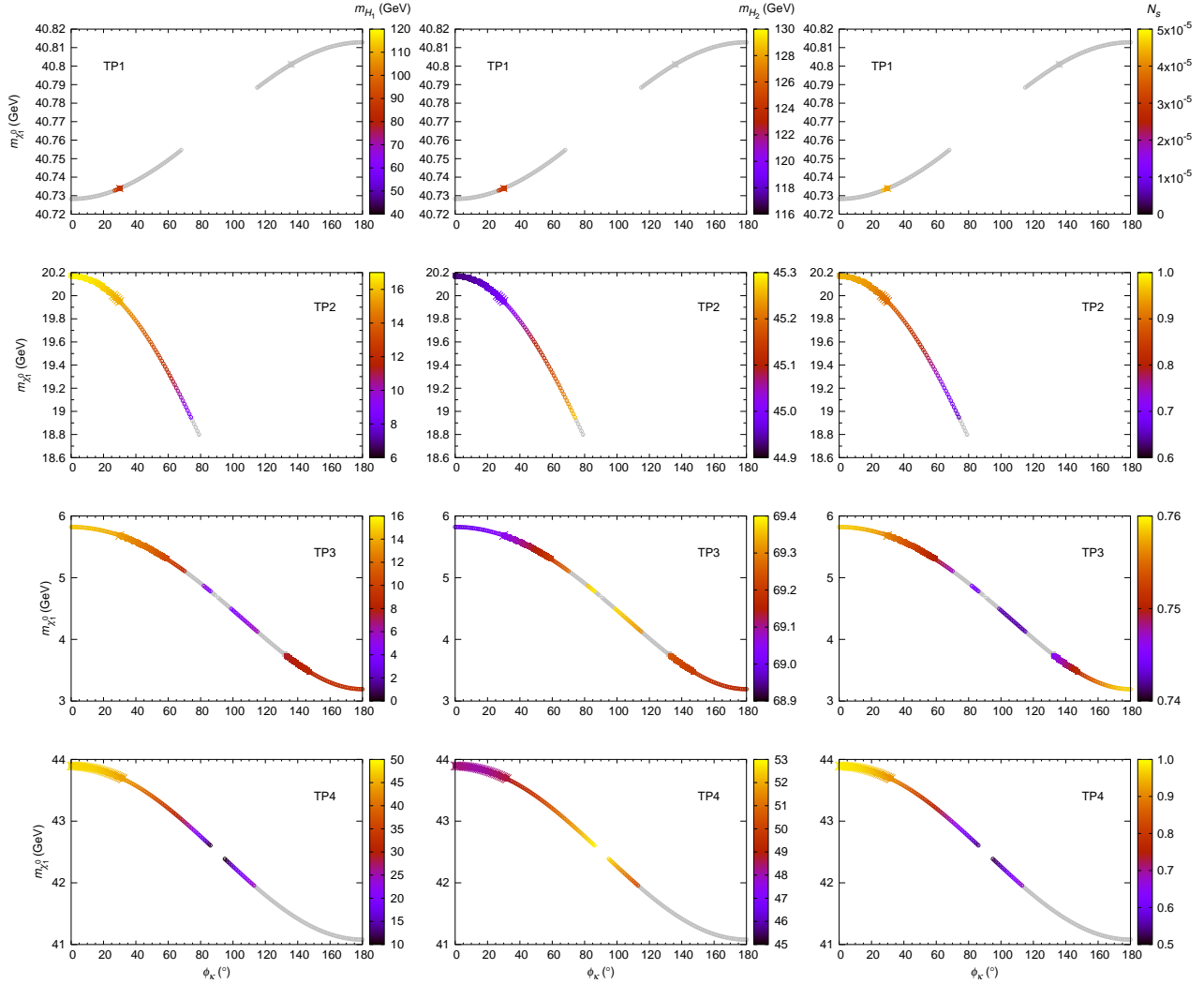


Figure 3: $m_{\tilde{\chi}_1^0}$ as a function of ϕ_κ for the test points 1 (top row) – 4 (bottom row). The heat maps correspond to m_{H_1} (left column), m_{H_2} (central column) and N_s (right column). The grey circles imply inconsistency with one of the experimental constraints, while the coloured circles give $\Omega_{\tilde{\chi}_1^0} h^2 > 0.131$. The coloured boxes correspond to $\Omega_{\tilde{\chi}_1^0} h^2 < 0.131$, and a cross around a box implies $0.107 < \Omega_{\tilde{\chi}_1^0} h^2 < 0.131$, besides consistency with all the other constraints.

$\text{BR}(H_{\text{SM}} \rightarrow H_2 H_2)$ rises from about 8% to about about 18%. Overall then, the phenomenology of the 4-body final states with invariant mass near that of $H_{\text{SM}} = H_3$ for points analogous to the TP4 could be crucial for distinguishing the signatures of CP-conserving versus the CP-violating NMSSM. It will be the subject of a follow-up analysis.

Finally, we briefly comment on the possible LHC constraints on the EW sector of the model. Various searches targeting $\tilde{\chi}_1^\pm$ and $\tilde{\chi}_2^0$ production, such as [96, 97, 98], are relevant since both states can decay to our (very) light $\tilde{\chi}_1^0$ along with $W/Z/H_{\text{obs}}$. These analysis quote limits of up to 750 GeV, which are, however, for *winos* with specific channels of decay. Searches for higgsinos are notoriously difficult due to their small production cross-section, and greatly weaken the limits (the very latest ATLAS search [99] quotes limits of up to 210 GeV). Since the $\tilde{\chi}_1^\pm/\tilde{\chi}_2^0$ in TP1 and TP4 are rather

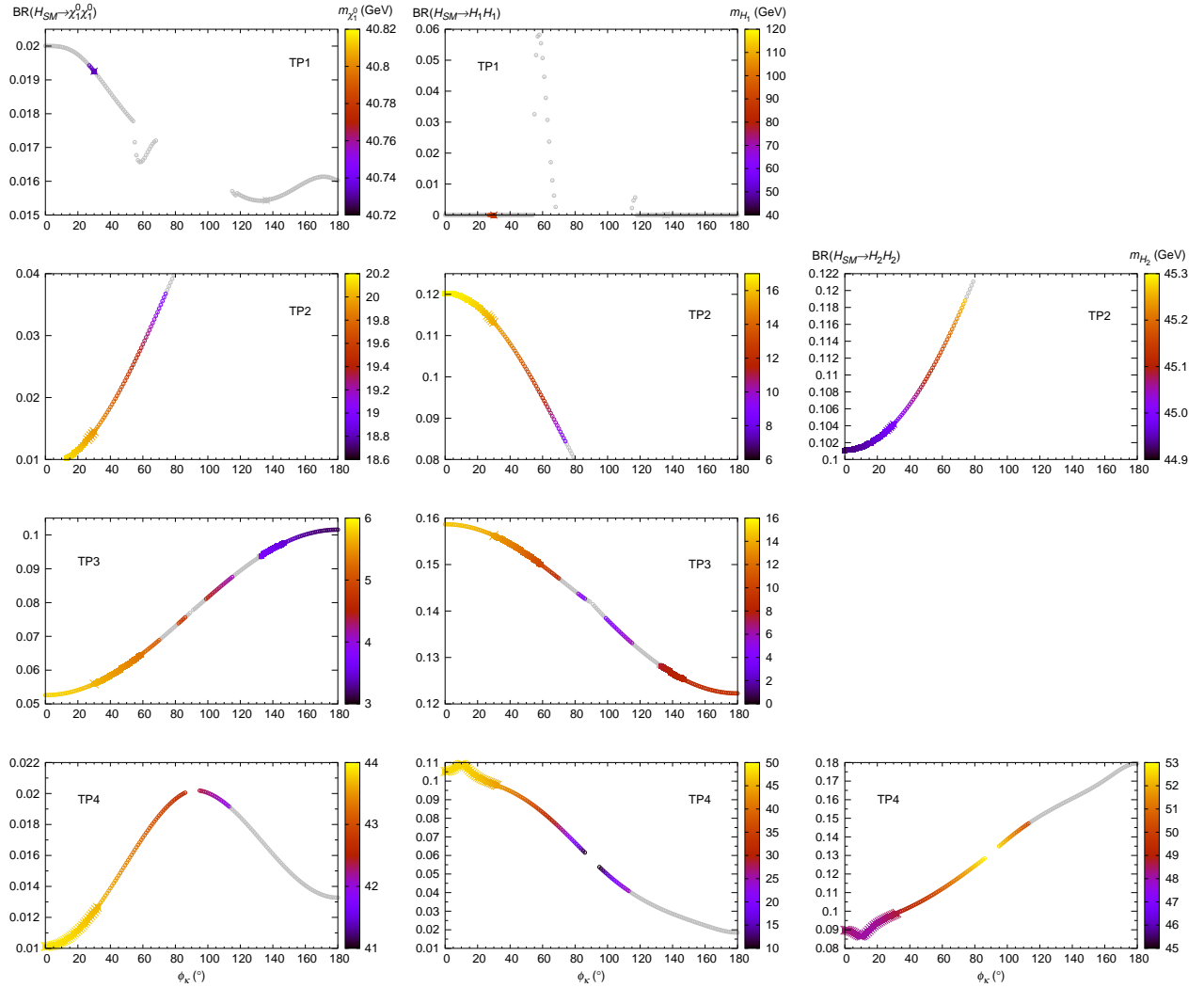


Figure 4: $\text{BR}(H_{\text{SM}} \rightarrow \tilde{\chi}_1^0 \tilde{\chi}_1^0)$ (left column), $\text{BR}(H_{\text{SM}} \rightarrow H_1 H_1)$ (central column), and $\text{BR}(H_{\text{SM}} \rightarrow H_2 H_2)$ (right column), as functions of ϕ_κ for the TPs 1 (top row) – 4 (bottom row). The colour maps in the left, central and right columns correspond to $m_{\tilde{\chi}_1^0}$, m_{H_1} and m_{H_2} , respectively.

heavy, we believe that they should escape all current searches. For TP2 and TP3 they should evade the current limits because instead of decaying to $W/Z/H_{\text{obs}}$, our $\tilde{\chi}_2^0$ can decay dominantly to the lighter singlet-like Higgs boson. Nevertheless, in our follow-up analysis it would be interesting to test our scan points against latest results using a fast tool such as `SModelS` [100, 101, 102, 103, 104] and to process a handful using full recasting in `MadAnalysis` [105, 106, 107, 108] with the latest searches in [109, 110] (see also [111] for a review of available recasting tools), as performed in, e.g., [112].

5 Summary and conclusions

The Higgs sector of the NMSSM can accommodate explicit CP-violating phases at the tree level, whereas in the MSSM such phases enter the Higgs potential only at the higher orders. While the

measurements of the leptonic EDMs tightly bound the MSSM-like phase in $A_{\tilde{f}}$, radiatively induced from the sfermion sector, they have been previously found to be much less constraining of the phase of κ . Importantly, this phase also appears in the tree-level mass term, $2\kappa s$, corresponding to the singlino interaction eigenstate. Therefore, if the $\tilde{\chi}_1^0$ is singlino-dominated, its relic abundance can have a strong dependence on ϕ_κ .

The cNMSSM contains 5 neutral CP-indefinite Higgs bosons in total, and any one (or more) of the three lightest of these can fulfil the role of the H_{SM} , in specific regions of the model’s parameter space. In this study, we have analysed in detail the quantitative impact of the variation in ϕ_κ on $\Omega_{\tilde{\chi}_1^0} h^2$, for scenarios wherein either $H_{\text{SM}} = H_2$ or $H_{\text{SM}} = H_3$. The H_1 was required to always be lighter than 125 GeV to increase the prospects of self-annihilation of the singlino-like $\tilde{\chi}_1^0$ solutions with mass $\lesssim 100$ GeV, which was our main focus. For certain select values of ϕ_κ , we performed numerical scans of the free parameters of the EW-scale cNMSSM, to find points consistent with a variety of recent experimental constraints, in particular the electron EDM.

In the overall picture that emerges from this analysis, for specific values of ϕ_κ , nearly exact consistency with the Planck measurement of the DM relic abundance of the Universe is seen for certain $m_{\tilde{\chi}_1^0}$ that are precluded in the real NMSSM. Thus, while a large gap appears near $\Omega_{\tilde{\chi}_1^0} h^2 \approx 0.119$ for $m_{\tilde{\chi}_1^0} \sim 10 - 30$ GeV for $\phi_\kappa = 0^\circ$, this mass range starts filling up as the CP-violation increases, and gets almost entirely covered for $\phi_\kappa \sim 135^\circ$. Evidently, this results from the subtle tweaks in the composition of $\tilde{\chi}_1^0$, so that its couplings allow just the right amount of its self-annihilation via one of the multiple potentially resonant sources available in this model, when the CP-violation is turned on.

This inference was confirmed by a closer investigation of the four test points selected out of the successful points from the scans. For each of these points we varied ϕ_κ over the entire $0^\circ - 180^\circ$, while fixing the other nine free parameters to their original values. This demonstrated how the different values of ϕ_κ modify m_{H_1} and m_{H_2} , besides the mass as well as the N_s of the $\tilde{\chi}_1^0$, to impact the consistency of these points not only with Ωh^2 but also with other experimental data. Furthermore, magnitudes of observables like the $\text{BR}(H_{\text{SM}} \rightarrow \tilde{\chi}_1^0 \tilde{\chi}_1^0)$, the $\text{BR}(H_{\text{SM}} \rightarrow H_1 H_1)$ and the $\text{BR}(H_{\text{SM}} \rightarrow H_2 H_2)$ also show a dependence on ϕ_κ significant enough that their dedicated inspection might help identify signatures of CP-violation in the NMSSM at the LHC.

Acknowledgments

The authors thank Shabbar Raza for his collaboration in the early stages of this project. MDG acknowledges support from the ‘‘HiggsAutomator’’ (ANR-15-CE31-0002) and ‘‘DMwithLLPatLHC’’ grants of the Agence Nationale de la Recherche (ANR).

References

- [1] H. P. Nilles, *Supersymmetry, Supergravity and Particle Physics*, *Phys. Rept.* **110** (1984) 1–162.
- [2] H. E. Haber and G. L. Kane, *The Search for Supersymmetry: Probing Physics Beyond the Standard Model*, *Phys. Rept.* **117** (1985) 75–263.
- [3] ATLAS collaboration, G. Aad et al., *Observation of a new particle in the search for the Standard Model Higgs boson with the ATLAS detector at the LHC*, *Phys.Lett.* **B716** (2012) 1–29, [1207.7214].

- [4] CMS collaboration, S. Chatrchyan et al., *Observation of a New Boson at a Mass of 125 GeV with the CMS Experiment at the LHC*, *Phys. Lett. B* **716** (2012) 30–61, [1207.7235].
- [5] CMS collaboration, S. Chatrchyan et al., *Observation of a new boson with mass near 125 GeV in pp collisions at $\sqrt{s} = 7$ and 8 TeV*, *JHEP* **1306** (2013) 081, [1303.4571].
- [6] A. Djouadi, *The Anatomy of electro-weak symmetry breaking. II. The Higgs bosons in the minimal supersymmetric model*, *Phys. Rept.* **459** (2008) 1–241, [hep-ph/0503173].
- [7] P. Bergeron and S. Profumo, *IceCube, DeepCore, PINGU and the indirect search for supersymmetric dark matter*, *JCAP* **01** (2014) 026, [1312.4445].
- [8] L. Roszkowski, E. M. Sessolo and S. Trojanowski, *WIMP dark matter candidates and searches – current status and future prospects*, *Rept. Prog. Phys.* **81** (2018) 066201, [1707.06277].
- [9] P. Fayet, *Supergauge Invariant Extension of the Higgs Mechanism and a Model for the electron and Its Neutrino*, *Nucl. Phys.* **B90** (1975) 104–124.
- [10] J. R. Ellis, J. Gunion, H. E. Haber, L. Roszkowski and F. Zwirner, *Higgs Bosons in a Nonminimal Supersymmetric Model*, *Phys. Rev.* **D39** (1989) 844.
- [11] L. Durand and J. L. Lopez, *Upper Bounds on Higgs and Top Quark Masses in the Flipped $SU(5) \times U(1)$ Superstring Model*, *Phys. Lett.* **B217** (1989) 463.
- [12] M. Drees, *Supersymmetric Models with Extended Higgs Sector*, *Int. J. Mod. Phys.* **A4** (1989) 3635.
- [13] U. Ellwanger, C. Hugonie and A. M. Teixeira, *The Next-to-Minimal Supersymmetric Standard Model*, *Phys. Rept.* **496** (2010) 1–77, [0910.1785].
- [14] M. Maniatis, *The Next-to-Minimal Supersymmetric extension of the Standard Model reviewed*, *Int. J. Mod. Phys.* **A25** (2010) 3505–3602, [0906.0777].
- [15] N.-E. Bomark, S. Moretti, S. Munir and L. Roszkowski, *A light NMSSM pseudoscalar Higgs boson at the LHC redux*, *JHEP* **02** (2015) 044, [1409.8393].
- [16] S. A. Abel, S. Sarkar and I. B. Whittingham, *Neutralino dark matter in a class of unified theories*, *Nucl. Phys. B* **392** (1993) 83–110, [hep-ph/9209292].
- [17] J. Kozaczkuk and S. Profumo, *Light NMSSM neutralino dark matter in the wake of CDMS II and a 126 GeV Higgs boson*, *Phys. Rev. D* **89** (2014) 095012, [1308.5705].
- [18] J. Cao, C. Han, L. Wu, P. Wu and J. M. Yang, *A light SUSY dark matter after CDMS-II, LUX and LHC Higgs data*, *JHEP* **05** (2014) 056, [1311.0678].
- [19] T. Han, Z. Liu and S. Su, *Light Neutralino Dark Matter: Direct/Indirect Detection and Collider Searches*, *JHEP* **08** (2014) 093, [1406.1181].
- [20] U. Ellwanger and C. Hugonie, *The semi-constrained NMSSM satisfying bounds from the LHC, LUX and Planck*, *JHEP* **08** (2014) 046, [1405.6647].
- [21] D. Das, U. Ellwanger and A. M. Teixeira, *Modified Signals for Supersymmetry in the NMSSM with a Singlino-like LSP*, *JHEP* **04** (2012) 067, [1202.5244].

- [22] U. Ellwanger, *Testing the higgsino-singlino sector of the NMSSM with trileptons at the LHC*, *JHEP* **11** (2013) 108, [1309.1665].
- [23] J. S. Kim and T. S. Ray, *The higgsino-singlino world at the large hadron collider*, *Eur. Phys. J. C* **75** (2015) 40, [1405.3700].
- [24] U. Ellwanger and A. M. Teixeira, *NMSSM with a singlino LSP: possible challenges for searches for supersymmetry at the LHC*, *JHEP* **10** (2014) 113, [1406.7221].
- [25] C. Han, D. Kim, S. Munir and M. Park, *$\mathcal{O}(1)$ GeV dark matter in SUSY and a very light pseudoscalar at the LHC*, *JHEP* **07** (2015) 002, [1504.05085].
- [26] C. T. Potter, *Natural NMSSM with a Light Singlet Higgs and Singlino LSP*, *Eur. Phys. J. C* **76** (2016) 44, [1505.05554].
- [27] R. Enberg, S. Munir, C. Pérez de los Heros and D. Werder, *Prospects for higgsino-singlino dark matter detection at IceCube and PINGU*, 1506.05714.
- [28] U. Ellwanger, *Present Status and Future Tests of the Higgsino-Singlino Sector in the NMSSM*, *JHEP* **02** (2017) 051, [1612.06574].
- [29] F. Domingo, J. S. Kim, V. M. Lozano, P. Martin-Ramiro and R. Ruiz de Austri, *Confronting the neutralino and chargino sector of the NMSSM with the multilepton searches at the LHC*, *Phys. Rev. D* **101** (2020) 075010, [1812.05186].
- [30] U. Ellwanger and C. Hugonie, *The higgsino-singlino sector of the NMSSM: combined constraints from dark matter and the LHC*, *Eur. Phys. J. C* **78** (2018) 735, [1806.09478].
- [31] F. Ferrer, L. M. Krauss and S. Profumo, *Indirect detection of light neutralino dark matter in the NMSSM*, *Phys. Rev. D* **74** (2006) 115007, [hep-ph/0609257].
- [32] S. Demidov and O. Suvorova, *Annihilation of NMSSM neutralinos in the Sun and neutrino telescope limits*, *JCAP* **06** (2010) 018, [1006.0872].
- [33] A. Sakharov, *Violation of CP Invariance, c Asymmetry, and Baryon Asymmetry of the Universe*, *Pisma Zh. Eksp. Teor. Fiz.* **5** (1967) 32–35.
- [34] A. G. Cohen, D. Kaplan and A. Nelson, *Progress in electroweak baryogenesis*, *Ann. Rev. Nucl. Part. Sci.* **43** (1993) 27–70, [hep-ph/9302210].
- [35] M. Quiros, *Field theory at finite temperature and phase transitions*, *Helv. Phys. Acta* **67** (1994) 451–583.
- [36] V. Rubakov and M. Shaposhnikov, *Electroweak baryon number nonconservation in the early universe and in high-energy collisions*, *Usp. Fiz. Nauk* **166** (1996) 493–537, [hep-ph/9603208].
- [37] M. Trodden, *Electroweak baryogenesis*, *Rev. Mod. Phys.* **71** (1999) 1463–1500, [hep-ph/9803479].
- [38] A. Pilaftsis, *CP odd tadpole renormalization of Higgs scalar - pseudoscalar mixing*, *Phys. Rev. D* **58** (1998) 096010, [hep-ph/9803297].

- [39] A. Pilaftsis, *Higgs scalar - pseudoscalar mixing in the minimal supersymmetric standard model*, *Phys. Lett.* **B435** (1998) 88–100, [[hep-ph/9805373](#)].
- [40] A. Pilaftsis and C. E. Wagner, *Higgs bosons in the minimal supersymmetric standard model with explicit CP violation*, *Nucl. Phys.* **B553** (1999) 3–42, [[hep-ph/9902371](#)].
- [41] M. S. Carena, J. R. Ellis, A. Pilaftsis and C. Wagner, *Renormalization group improved effective potential for the MSSM Higgs sector with explicit CP violation*, *Nucl. Phys.* **B586** (2000) 92–140, [[hep-ph/0003180](#)].
- [42] S. Choi, M. Drees and J. S. Lee, *Loop corrections to the neutral Higgs boson sector of the MSSM with explicit CP violation*, *Phys. Lett.* **B481** (2000) 57–66, [[hep-ph/0002287](#)].
- [43] M. S. Carena, J. R. Ellis, A. Pilaftsis and C. Wagner, *Higgs boson pole masses in the MSSM with explicit CP violation*, *Nucl. Phys.* **B625** (2002) 345–371, [[hep-ph/0111245](#)].
- [44] M. S. Carena, J. R. Ellis, S. Mrenna, A. Pilaftsis and C. Wagner, *Collider probes of the MSSM Higgs sector with explicit CP violation*, *Nucl. Phys.* **B659** (2003) 145–178, [[hep-ph/0211467](#)].
- [45] S. Choi, J. Kalinowski, Y. Liao and P. Zerwas, *H/A Higgs mixing in CP-noninvariant supersymmetric theories*, *Eur. Phys. J.* **C40** (2005) 555–564, [[hep-ph/0407347](#)].
- [46] M. Frank, T. Hahn, S. Heinemeyer, W. Hollik, H. Rzehak and G. Weiglein, *The Higgs Boson Masses and Mixings of the Complex MSSM in the Feynman-Diagrammatic Approach*, *JHEP* **02** (2007) 047, [[hep-ph/0611326](#)].
- [47] S. Heinemeyer, W. Hollik, H. Rzehak and G. Weiglein, *The Higgs sector of the complex MSSM at two-loop order: QCD contributions*, *Phys. Lett.* **B652** (2007) 300–309, [[0705.0746](#)].
- [48] M. S. Carena, J. R. Ellis, A. Pilaftsis and C. Wagner, *CP violating MSSM Higgs bosons in the light of LEP-2*, *Phys. Lett.* **B495** (2000) 155–163, [[hep-ph/0009212](#)].
- [49] S. Abel, S. Khalil and O. Lebedev, *EDM constraints in supersymmetric theories*, *Nucl. Phys.* **B606** (2001) 151–182, [[hep-ph/0103320](#)].
- [50] M. D. Goodsell and F. Staub, *The Higgs mass in the CP violating MSSM, NMSSM, and beyond*, *Eur. Phys. J.* **C77** (2017) 46, [[1604.05335](#)].
- [51] R. Grober, M. Muhlleitner and M. Spira, *Higgs Pair Production at NLO QCD for CP-violating Higgs Sectors*, *Nucl. Phys. B* **925** (2017) 1–27, [[1705.05314](#)].
- [52] T. N. Dao, R. Gröber, M. Krause, M. Mühlleitner and H. Rzehak, *Two-loop $\mathcal{O}(\alpha_t^2)$ corrections to the neutral Higgs boson masses in the CP-violating NMSSM*, *JHEP* **08** (2019) 114, [[1903.11358](#)].
- [53] T. N. Dao, M. Mühlleitner, S. Patel and K. Sakurai, *One-loop Corrections to the Two-Body Decays of the Charged Higgs Bosons in the Real and Complex NMSSM*, *Eur. Phys. J.* **C81** (2021) 340, [[2012.14889](#)].
- [54] F. Domingo and S. Paßehr, *Fighting off field dependence in MSSM Higgs-mass corrections of order $\alpha_t \alpha_s$ and α_t^2* , *Eur. Phys. J.* **C81** (2021) 661, [[2105.01139](#)].

- [55] T. N. Dao, M. Gabelmann, M. Mühlleitner and H. Rzehak, *Two-loop $\mathcal{O}((\alpha_t + \alpha_\lambda + \alpha_\kappa)^2)$ corrections to the Higgs boson masses in the CP-violating NMSSM*, *JHEP* **09** (2021) 193, [2106.06990].
- [56] P. Slavich et al., *Higgs-mass predictions in the MSSM and beyond*, *Eur. Phys. J. C* **81** (2021) 450, [2012.15629].
- [57] T. Graf, R. Grober, M. Mühlleitner, H. Rzehak and K. Walz, *Higgs Boson Masses in the Complex NMSSM at One-Loop Level*, *JHEP* **1210** (2012) 122, [1206.6806].
- [58] S. Moretti, S. Munir and P. Poulose, *125 GeV Higgs Boson signal within the complex NMSSM*, *Phys. Rev.* **D89** (2014) 015022, [1305.0166].
- [59] S. Munir, *Novel Higgs-to-125 GeV Higgs boson decays in the complex NMSSM*, *Phys. Rev.* **D89** (2014) 095013, [1310.8129].
- [60] S. F. King, M. Mühlleitner, R. Nevzorov and K. Walz, *Exploring the CP-violating NMSSM: EDM Constraints and Phenomenology*, *Nucl. Phys. B* **901** (2015) 526–555, [1508.03255].
- [61] S. Moretti and S. Munir, *Two Higgs Bosons near 125 GeV in the Complex NMSSM and the LHC Run I Data*, *Adv. High Energy Phys.* **2015** (2015) 509847, [1505.00545].
- [62] B. Das, S. Moretti, S. Munir and P. Poulose, *Two Higgs bosons near 125 GeV in the NMSSM: beyond the narrow width approximation*, *Eur. Phys. J. C* **77** (2017) 544, [1704.02941].
- [63] F. Domingo, *A New Tool for the study of the CP-violating NMSSM*, *JHEP* **06** (2015) 052, [1503.07087].
- [64] D. J. Miller, R. Nevzorov and P. M. Zerwas, *The Higgs sector of the next-to-minimal supersymmetric standard model*, *Nucl. Phys.* **B681** (2004) 3–30, [hep-ph/0304049].
- [65] ACME collaboration, V. Andreev et al., *Improved limit on the electric dipole moment of the electron*, *Nature* **562** (2018) 355–360.
- [66] nEDM collaboration, C. Abel et al., *Measurement of the permanent electric dipole moment of the neutron*, *Phys. Rev. Lett.* **124** (2020) 081803, [2001.11966].
- [67] W. B. Cairncross, D. N. Gresh, M. Grau, K. C. Cossel, T. S. Roussy, Y. Ni et al., *Precision Measurement of the Electron’s Electric Dipole Moment Using Trapped Molecular Ions*, *Phys. Rev. Lett.* **119** (2017) 153001, [1704.07928].
- [68] W. C. Griffith, M. D. Swallows, T. H. Loftus, M. V. Romalis, B. R. Heckel and E. N. Fortson, *Improved Limit on the Permanent Electric Dipole Moment of Hg-199*, *Phys. Rev. Lett.* **102** (2009) 101601, [0901.2328].
- [69] B. C. Regan, E. D. Commins, C. J. Schmidt and D. DeMille, *New limit on the electron electric dipole moment*, *Phys. Rev. Lett.* **88** (2002) 071805.
- [70] K. Cheung, T.-J. Hou, J. S. Lee and E. Senaha, *The Higgs Boson Sector of the Next-to-MSSM with CP Violation*, *Phys. Rev.* **D82** (2010) 075007, [1006.1458].

- [71] K. Cheung, T.-J. Hou, J. S. Lee and E. Senaha, *Higgs Mediated EDMs in the Next-to-MSSM: An Application to Electroweak Baryogenesis*, *Phys. Rev.* **D84** (2011) 015002, [1102.5679].
- [72] W. Porod, *SPheno, a program for calculating supersymmetric spectra, SUSY particle decays and SUSY particle production at e^+e^- colliders*, *Comput. Phys. Commun.* **153** (2003) 275–315, [hep-ph/0301101].
- [73] W. Porod and F. Staub, *SPheno 3.1: Extensions including flavour, CP-phases and models beyond the MSSM*, *Comput. Phys. Commun.* **183** (2012) 2458–2469, [1104.1573].
- [74] F. Staub, *SARAH*, 0806.0538.
- [75] F. Staub, *SARAH 4: A tool for (not only SUSY) model builders*, *Comput. Phys. Commun.* **185** (2014) 1773–1790, [1309.7223].
- [76] M. D. Goodsell, K. Nickel and F. Staub, *Two-Loop Higgs mass calculations in supersymmetric models beyond the MSSM with SARAH and SPheno*, *Eur. Phys. J. C* **75** (2015) 32, [1411.0675].
- [77] M. Goodsell, K. Nickel and F. Staub, *Generic two-loop Higgs mass calculation from a diagrammatic approach*, *Eur. Phys. J. C* **75** (2015) 290, [1503.03098].
- [78] F. Staub, *Exploring new models in all detail with SARAH*, *Adv. High Energy Phys.* **2015** (2015) 840780, [1503.04200].
- [79] J. Braathen, M. D. Goodsell and F. Staub, *Supersymmetric and non-supersymmetric models without catastrophic Goldstone bosons*, *Eur. Phys. J. C* **77** (2017) 757, [1706.05372].
- [80] J. Baglio, R. Gröber, M. Mühlleitner, D. Nhung, H. Rzehak, M. Spira et al., *NMSSMCALC: A Program Package for the Calculation of Loop-Corrected Higgs Boson Masses and Decay Widths in the (Complex) NMSSM*, *Comput. Phys. Commun.* **185** (2014) 3372–3391, [1312.4788].
- [81] M. D. Goodsell, S. Liebler and F. Staub, *Generic calculation of two-body partial decay widths at the full one-loop level*, *Eur. Phys. J. C* **77** (2017) 758, [1703.09237].
- [82] F. Feroz, M. Hobson and M. Bridges, *MultiNest: an efficient and robust Bayesian inference tool for cosmology and particle physics*, *Mon. Not. Roy. Astron. Soc.* **398** (2009) 1601–1614, [0809.3437].
- [83] A. Belyaev, N. D. Christensen and A. Pukhov, *CalcHEP 3.4 for collider physics within and beyond the Standard Model*, *Comput. Phys. Commun.* **184** (2013) 1729–1769, [1207.6082].
- [84] G. Belanger, F. Boudjema, A. Pukhov and A. Semenov, *MicrOMEGAs 2.0: A Program to calculate the relic density of dark matter in a generic model*, *Comput. Phys. Commun.* **176** (2007) 367–382, [hep-ph/0607059].
- [85] G. Bélanger, F. Boudjema, A. Pukhov and A. Semenov, *MicrOMEGAs4.1: two dark matter candidates*, *Comput. Phys. Commun.* **192** (2015) 322–329, [1407.6129].
- [86] D. Barducci, G. Belanger, J. Bernon, F. Boudjema, J. Da Silva, S. Kraml et al., *Collider limits on new physics within micrOMEGAs-4.3*, *Comput. Phys. Commun.* **222** (2018) 327–338, [1606.03834].

- [87] ATLAS, CMS collaborations, J. M. Langford, *Combination of Higgs measurements from ATLAS and CMS : couplings and κ -framework*, *PoS LHCP2020* (2021) 136.
- [88] P. Bechtle, S. Heinemeyer, T. Klingl, T. Stefaniak, G. Weiglein and J. Wittbrodt, *HiggsSignals-2: Probing new physics with precision Higgs measurements in the LHC 13 TeV era*, 2012.09197.
- [89] HFLAV collaboration, Y. Amhis et al., *Averages of b-hadron, c-hadron, and τ -lepton properties as of summer 2016*, *Eur. Phys. J. C* **77** (2017) 895, [1612.07233].
- [90] LHCb collaboration, R. Aaij et al., *Measurement of the $B_s^0 \rightarrow \mu^+ \mu^-$ branching fraction and effective lifetime and search for $B^0 \rightarrow \mu^+ \mu^-$ decays*, *Phys. Rev. Lett.* **118** (2017) 191801, [1703.05747].
- [91] P. Bechtle, D. Dercks, S. Heinemeyer, T. Klingl, T. Stefaniak, G. Weiglein et al., *HiggsBounds-5: Testing Higgs Sectors in the LHC 13 TeV Era*, *Eur. Phys. J. C* **80** (2020) 1211, [2006.06007].
- [92] PLANCK collaboration, N. Aghanim et al., *Planck 2018 results. VI. Cosmological parameters*, *Astron. Astrophys.* **641** (2020) A6, [1807.06209].
- [93] B. S. Acharya, P. Kumar, K. Bobkov, G. Kane, J. Shao and S. Watson, *Non-thermal Dark Matter and the Moduli Problem in String Frameworks*, *JHEP* **06** (2008) 064, [0804.0863].
- [94] K. M. Zurek, *Multi-Component Dark Matter*, *Phys. Rev. D* **79** (2009) 115002, [0811.4429].
- [95] XENON collaboration, E. Aprile et al., *Dark Matter Search Results from a One Ton-Year Exposure of XENON1T*, *Phys. Rev. Lett.* **121** (2018) 111302, [1805.12562].
- [96] ATLAS collaboration, G. Aad et al., *Search for electroweak production of charginos and sleptons decaying into final states with two leptons and missing transverse momentum in $\sqrt{s} = 13$ TeV pp collisions using the ATLAS detector*, *Eur. Phys. J. C* **80** (2020) 123, [1908.08215].
- [97] ATLAS collaboration, G. Aad et al., *Search for direct production of electroweakinos in final states with one lepton, missing transverse momentum and a Higgs boson decaying into two b-jets in pp collisions at $\sqrt{s} = 13$ TeV with the ATLAS detector*, *Eur. Phys. J. C* **80** (2020) 691, [1909.09226].
- [98] ATLAS collaboration, G. Aad et al., *Search for chargino-neutralino production with mass splittings near the electroweak scale in three-lepton final states in $\sqrt{s}=13$ TeV pp collisions with the ATLAS detector*, *Phys. Rev. D* **101** (2020) 072001, [1912.08479].
- [99] ATLAS collaboration, G. Aad et al., *Search for chargino-neutralino pair production in final states with three leptons and missing transverse momentum in $\sqrt{s} = 13$ TeV pp collisions with the ATLAS detector*, *Eur. Phys. J. C* **81** (2021) 1118, [2106.01676].
- [100] S. Kraml, S. Kulkarni, U. Laa, A. Lessa, W. Magerl, D. Proschofsky-Spindler et al., *SModelS: a tool for interpreting simplified-model results from the LHC and its application to supersymmetry*, *Eur. Phys. J. C* **74** (2014) 2868, [1312.4175].
- [101] F. Ambrogio, S. Kraml, S. Kulkarni, U. Laa, A. Lessa, V. Magerl et al., *SModelS v1.1 user manual: Improving simplified model constraints with efficiency maps*, *Comput. Phys. Commun.* **227** (2018) 72–98, [1701.06586].

- [102] F. Ambrogio et al., *SModelS v1.2: long-lived particles, combination of signal regions, and other novelties*, *Comput. Phys. Commun.* **251** (2020) 106848, [1811.10624].
- [103] C. K. Khosa, S. Kraml, A. Lessa, P. Neuhuber and W. Waltenberger, *SModelS Database Update v1.2.3*, *LHEP* **2020** (2020) 158, [2005.00555].
- [104] G. Alguero, J. Heisig, C. Khosa, S. Kraml, S. Kulkarni, A. Lessa et al., *Constraining new physics with SModelS version 2*, 2112.00769.
- [105] E. Conte, B. Fuks and G. Serret, *MadAnalysis 5, A User-Friendly Framework for Collider Phenomenology*, *Comput. Phys. Comm.* **184** (2013) 222–256, [1206.1599].
- [106] E. Conte, B. Dumont, B. Fuks and C. Wymant, *Designing and recasting LHC analyses with MadAnalysis 5*, *Eur. Phys. J.* **C74** (2014) 3103, [1405.3982].
- [107] B. Dumont, B. Fuks, S. Kraml, S. Bein, G. Chalons, E. Conte et al., *Toward a public analysis database for LHC new physics searches using MADANALYSIS 5*, *Eur. Phys. J.* **C75** (2015) 56, [1407.3278].
- [108] E. Conte and B. Fuks, *Confronting new physics theories to LHC data with MADANALYSIS 5*, *Int. J. Mod. Phys.* **A33** (2018) 1830027, [1808.00480].
- [109] M. D. Goodsell, *Implementation of the ATLAS-SUSY-2019-08 analysis in the MadAnalysis 5 framework (electroweakinos with a Higgs decay into a $b\bar{b}$ pair, one lepton and missing transverse energy; 139/fb)*, *Mod. Phys. Lett. A* **36** (2021) 2141006.
- [110] B. Fuks et al., *Proceedings of the second MadAnalysis 5 workshop on LHC recasting in Korea*, *Mod. Phys. Lett. A* **36** (2021) 2102001, [2101.02245].
- [111] LHC REINTERPRETATION FORUM collaboration, W. Abdallah et al., *Reinterpretation of LHC Results for New Physics: Status and Recommendations after Run 2*, *SciPost Phys.* **9** (2020) 022, [2003.07868].
- [112] M. D. Goodsell, S. Kraml, H. Reyes-González and S. L. Williamson, *Constraining Electroweakinos in the Minimal Dirac Gaugino Model*, *SciPost Phys.* **9** (2020) 047, [2007.08498].